Electronic Supplementary Material (ESI) for Energy & Environmental Science.

Layered $LiTiO_2$ for Protection of Li_2S Cathodes Against Dissolution: Mechanisms of the Remarkable Performance Boost

Feixiang Wu[1], Travis P. Pollard[2], Enbo Zhao[1],Yiran Xiao[1], Marco Olguin,[2] Oleg Borodin[2]
and Gleb Yushin*[1]

[1] School of Materials Science and Engineering, Georgia Institute of Technology, Atlanta, GA 30332, USA.

[2] Electrochemistry Branch, Army Research Laboratory, Adelphi, MD 20783, USA.

*Corresponding author email: yushin@gatech.edu

Supplementary Figures

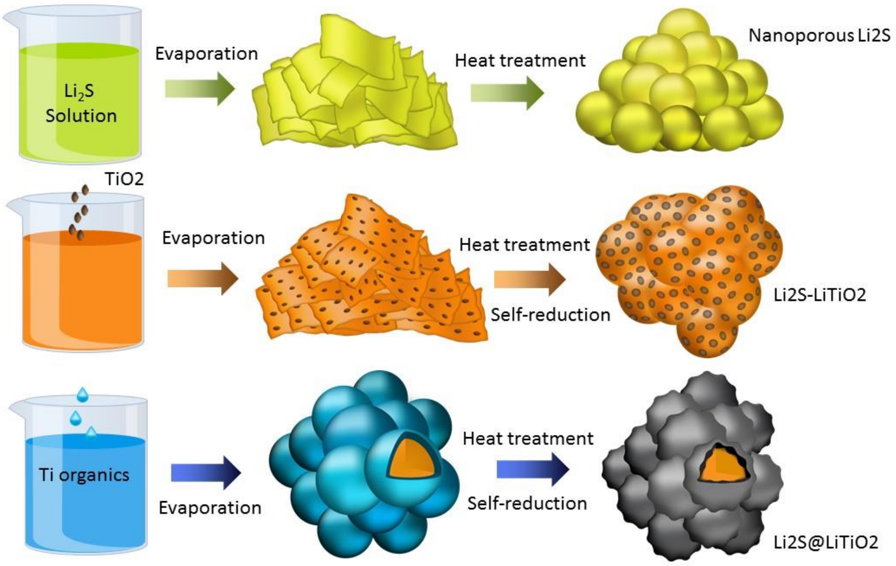

Figure S1 Schematic of the process flow for the scalable formation of regular Li_2S, Li_2S-$LiTiO_2$ and Li_2S@$LiTiO_2$ nanocomposite nanoparticles by two-steps: simple ethanol evaporation and then heat treatment in argon atmosphere.

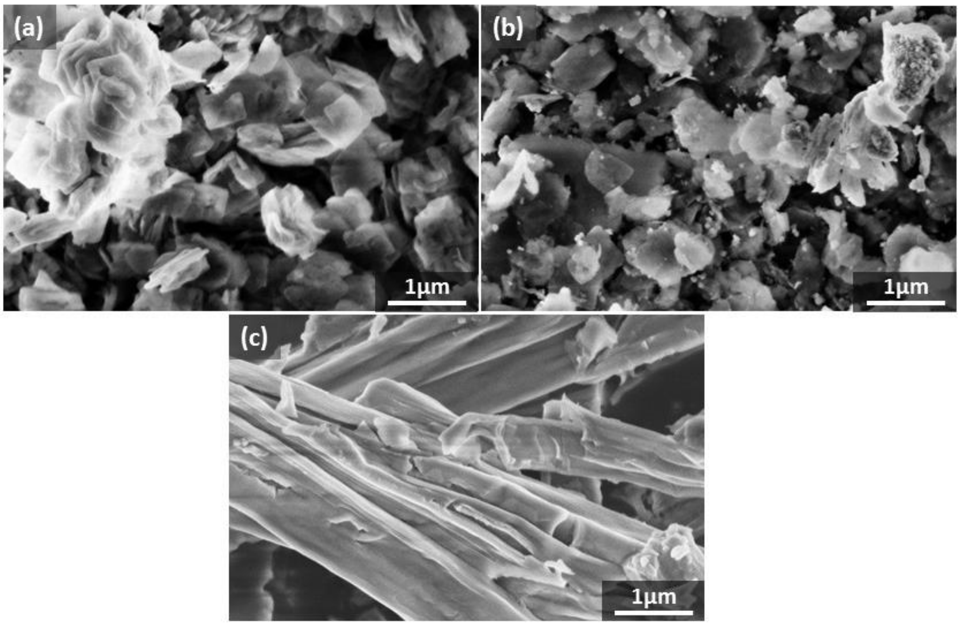

Figure S2 Characterization of the precursors of produced (a) regular Li_2S, (b) Li_2S-$LiTiO_2$ and (c) $Li_2S@LiTiO_2$ after ethanol evaporation.

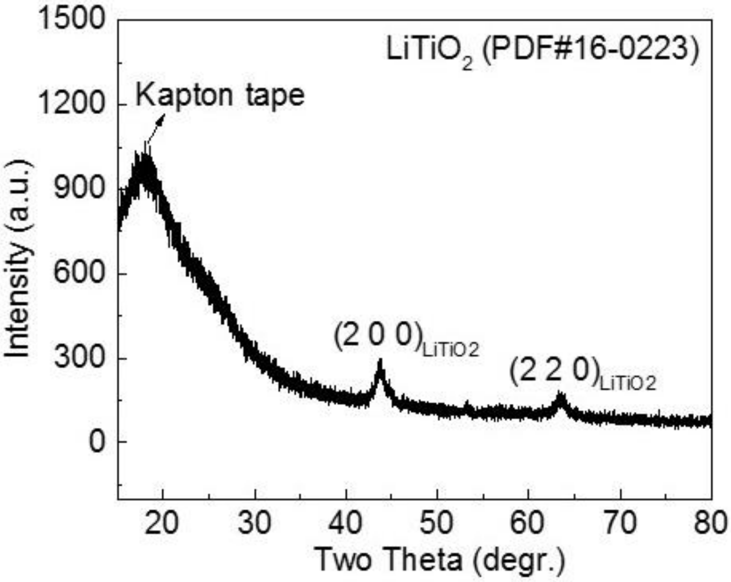

Figure S3 Characterization of the pure $LiTiO_2$: produced by Li_2S and TiO_2 (molar ratio is 1:2).

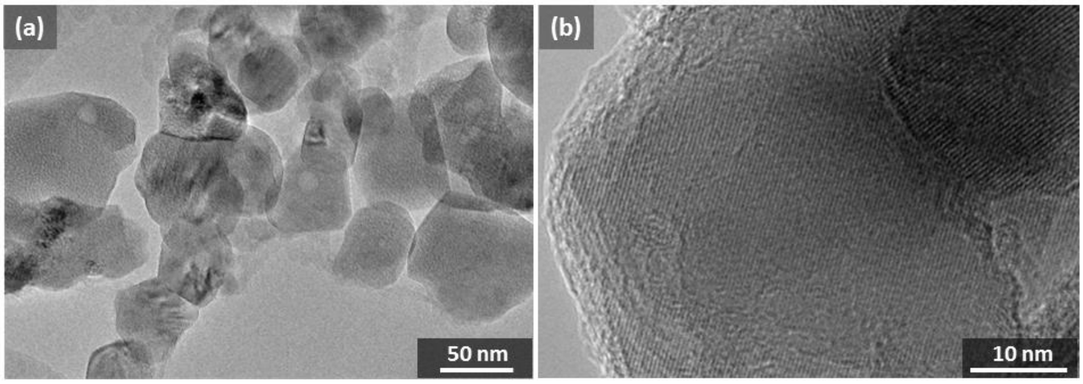

Figure S4 (a) TEM image and (b) HRTEM image of nanoporous Li_2S.

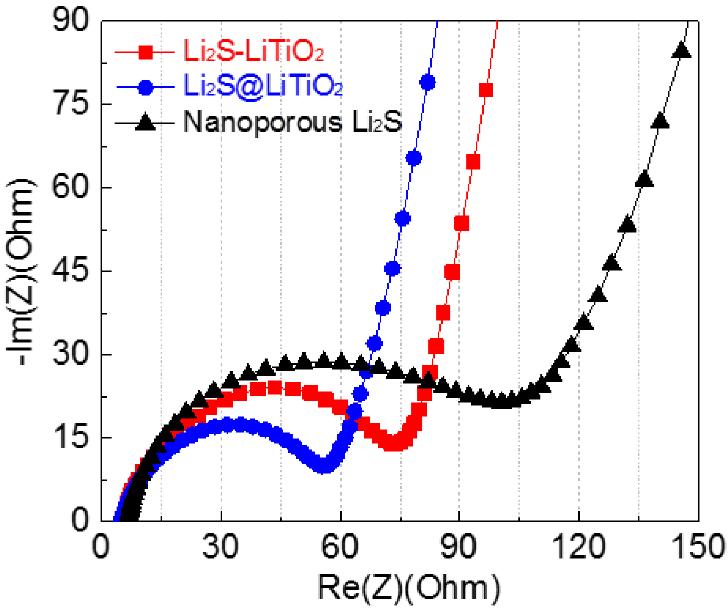

Figure S5 Comparison of impedance spectra in nanoporous Li_2S, Li_2S-$LiTiO_2$, and $Li_2S@LiTiO_2$ cells at the open-circuit voltage.

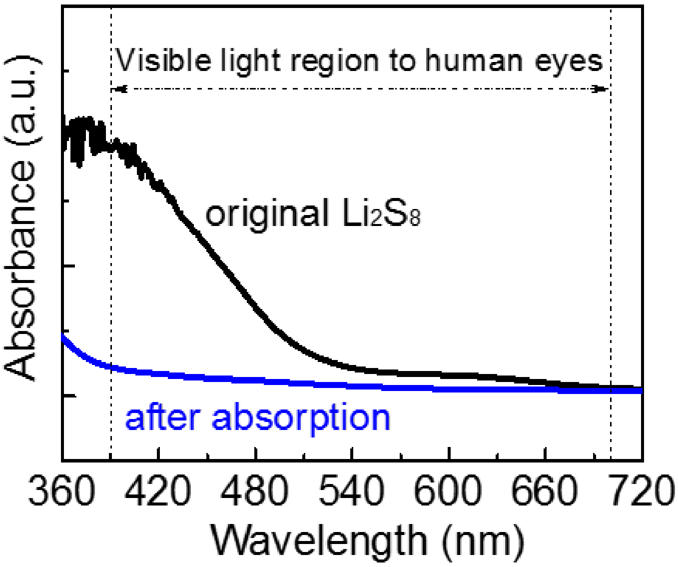

Figure S6 Ultraviolet-visible (UV-Vis) spectra data confirms anion (S_8^{2-}) adsorption (or decomposition) on the surface of $Li_2S@LiTiO_2$ nanoparticles.

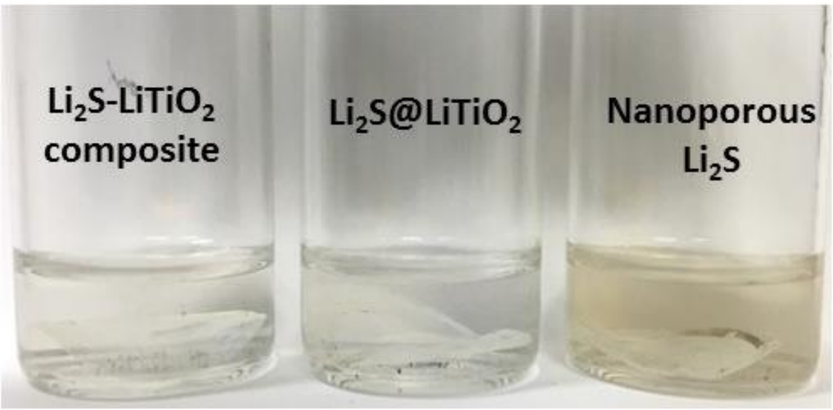

Figure S7 Cycled electrolytes with cycled separator inside (after 200 cycles) of the produced cathode-based cells.

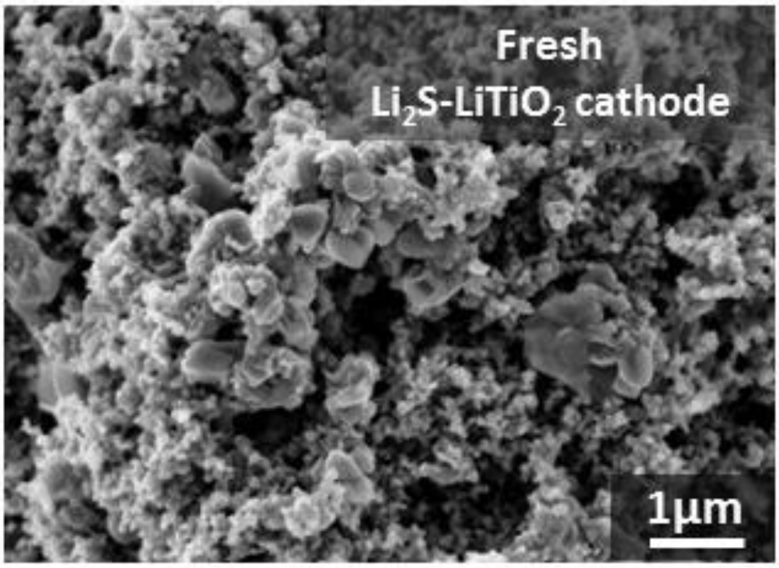

Figure S8 SEM image of fresh Li_2S-$LiTiO_2$ electrode.

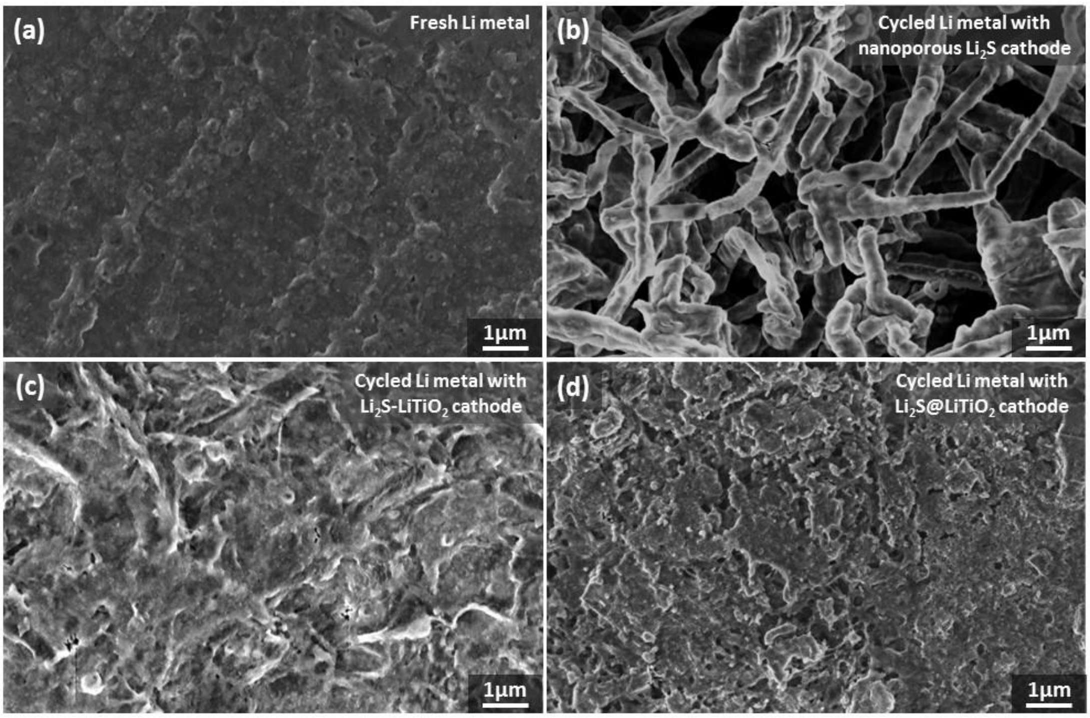

Figure S9 Characterization of the (a) fresh Li foil and (b, c, d) cycled Li foils after 200 cycles: (b) cycled Li metal in nanoporous Li_2S-based cell; (c) cycled Li metal in Li_2S-$LiTiO_2$-based cell; (d) cycled Li metal in Li_2S@$LiTiO_2$-based cell.

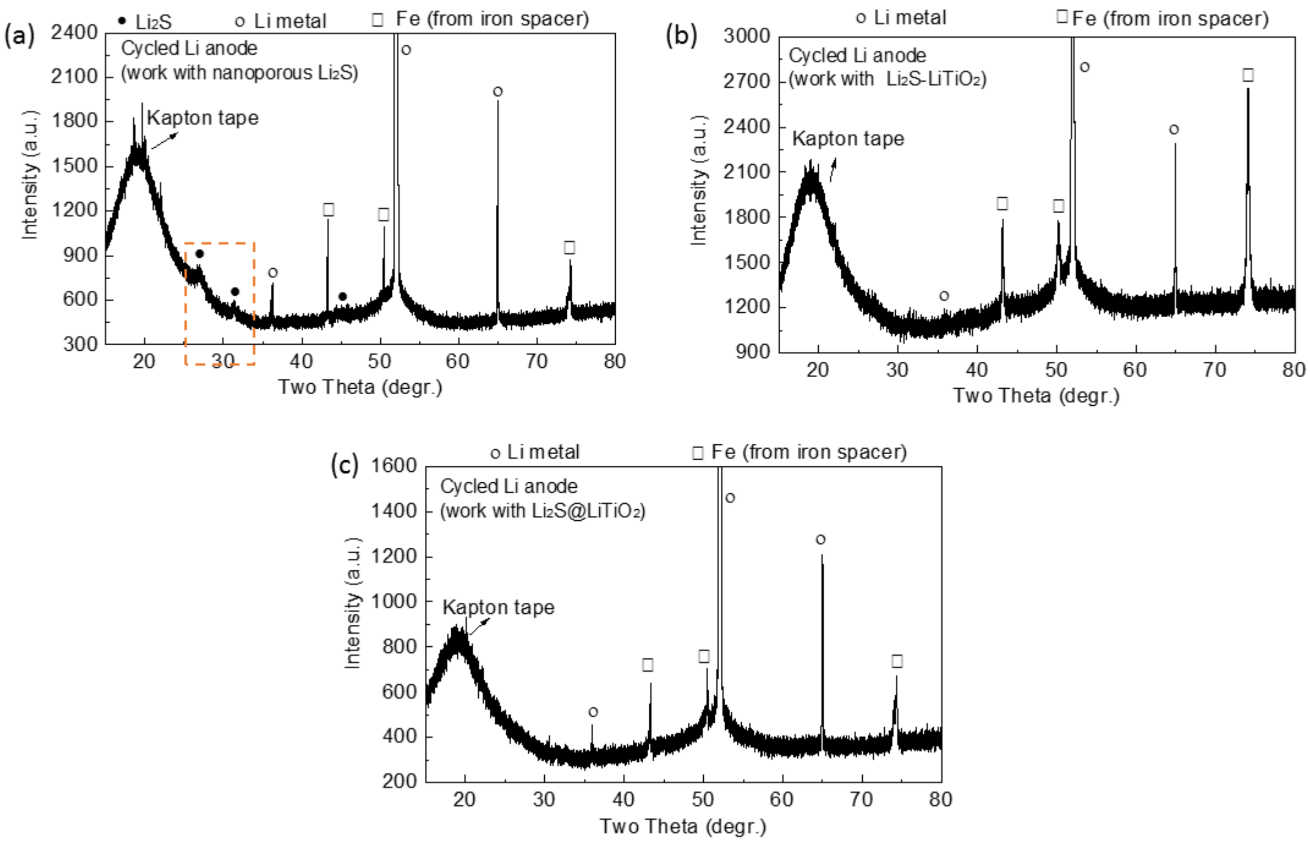

Figure S10 The comparison of XRD patterns of the cycled Li foils (200 cycles) in (a) nanoporous Li_2S, (b) Li_2S-$LiTiO_2$ and (c) Li_2S@$LiTiO_2$ cells, showing the lack of Li_2S precipitates on cycled Li foils in Li_2S-$LiTiO_2$ and Li_2S@$LiTiO_2$ cells.

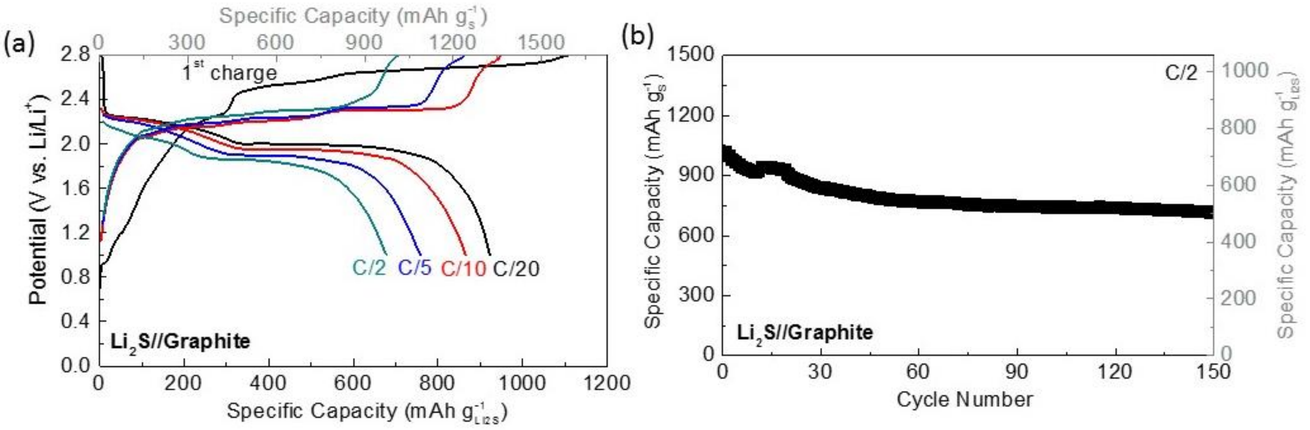

Figure S11 Li_2S@$LiTiO_2$//Graphite full cell studies: (a) charge-discharge profiles corresponding to different C-rates and (b) cycling performance in 150 cycles at C/2.

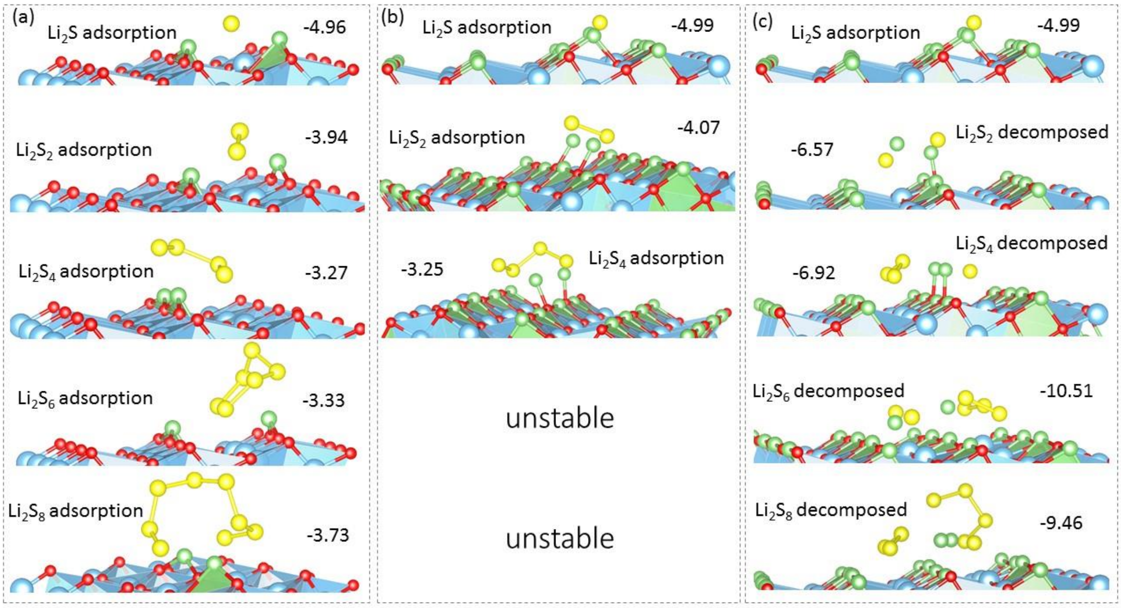

Figure S12 Optimized structures of Li_2S_X (X = 1, 2, 4, 6, 8; descending in each column) adsorbed on TiO_2 and $LiTiO_2$ substrates. Adsorption energies are listed in eV. Substrate surface in column (a) is TiO_2 and $LiTiO_2$ in columns (b) and (c). Column (b) shows local minima (for $X > 1$) where adsorbate remains intact and column (c) shows examples of the decomposition of the adsorbate material on the $LiTiO_2$ surface. Polysulfides of length $X > 4$ are found to be too reactive to adsorb without fragmentation on the $LiTiO_2$ surface. Color scheme: yellow (S), green (Li), blue (Ti), and red (O). Polyhedra colored by central atom.

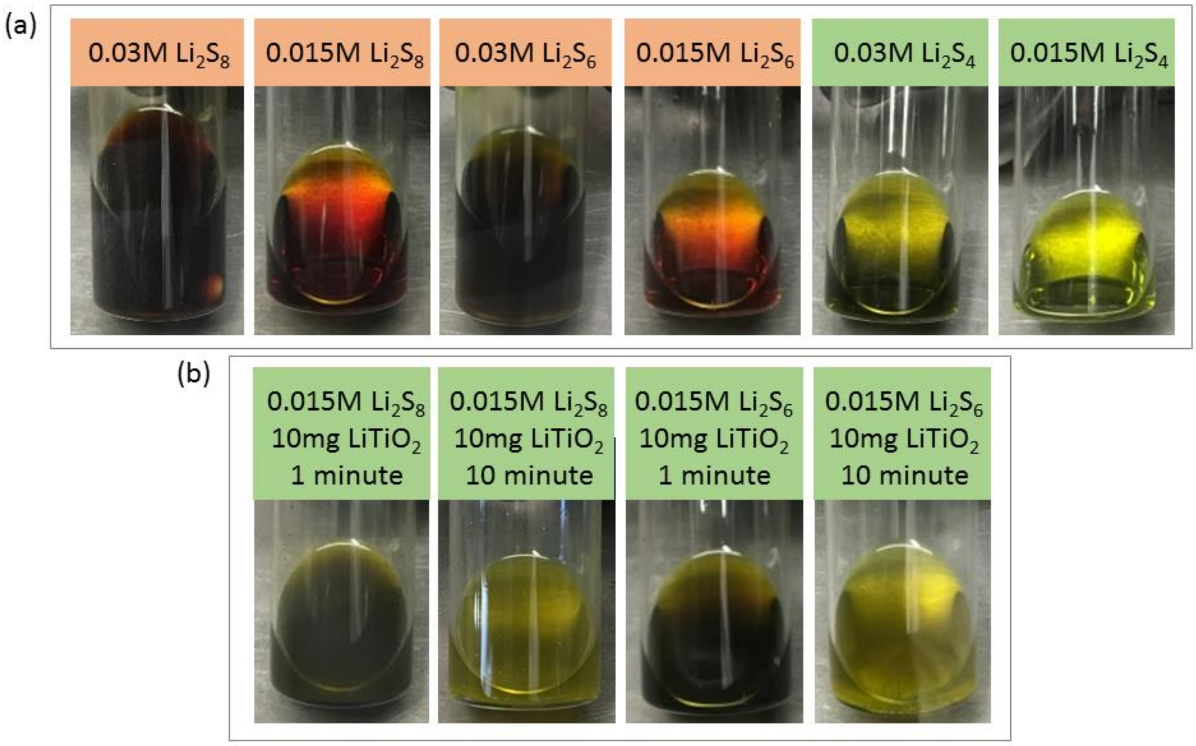

Figure S13 Chemical interactions between $LiTiO_2$ and long polysulfides: (a) prepared Li_2S_8, Li_2S_6 and Li_2S_4 solutions (0.015-0.03M in DME solvent), suggesting the orange-red color of Li_2S_8 and Li_2S_6 solutions, and yellow-green of Li_2S_4 solutions; (b) 10 mg of $LiTiO_2$ powder was added into 0.015M Li_2S_8 and 0.015M Li_2S_6 solutions, the color changed into yellow-green within one minute, suggesting the rapid conversion of longer polysulfides to short polysulfides on the surface of $LiTiO_2$.

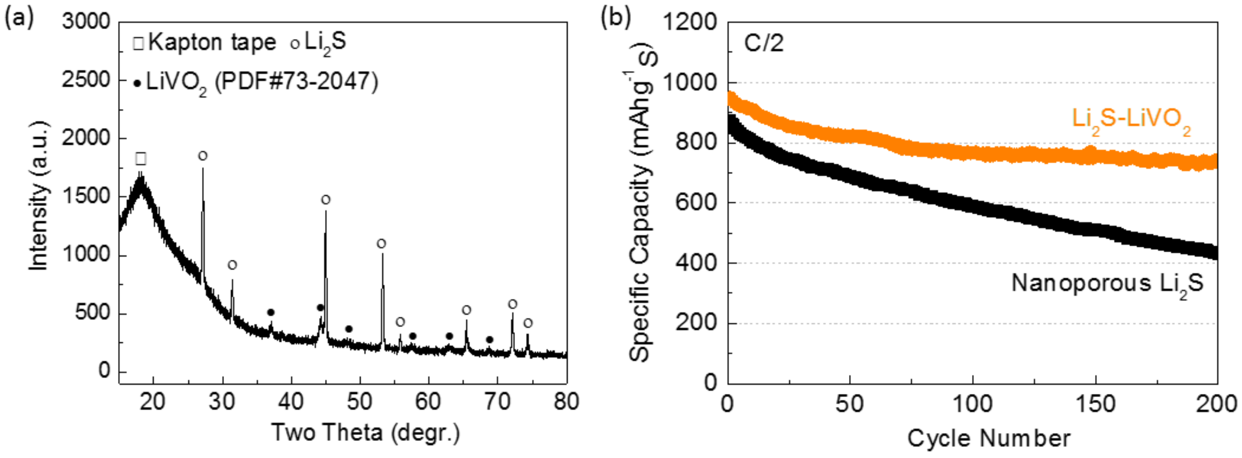

Figure S14 Showing the universality of our concept: it may work for all layered $LiMO_2$ and $LiMS_2$. We did the successful synthesis of the $LiVO_2$-Li_2S composite. (a) XRD result of the synthesized Li_2S-$LiVO_2$ composite; (b) The comparison of cycle stability at C/2 between nanoporous Li_2S and Li_2S-$LiVO_2$ cells.

Table S1 Comparison of the electrochemical performance of recent Li_2S-based cathodes.

Sample type	**Li_2S mass loading**	**Specific Capacity based on Li_2S**	**Cycling performance (capacity retention)**	**Reference**
Li_2S@C	1.0 mg·cm^{-2}	~410 mAh g^{-1} at 1C	~62% within 200cycles at 1C	[1]
Li_2S@C	1.0 mg·cm^{-2}	676 mAh g^{-1} at ~0.1C	~64% within 200cycles at ~0.1C	[2]
Li_2S@Ni-P-S@G	2.0 mg·cm^{-2}	~700 mAh g^{-1} at 0.5C	77.3% within 300cycles at 0.5C	[3]
Li_2S/N-doped G	1.8-2.3 mg cm^{-2}	657 mAh g^{-1} at 0.5C	~62% within 300cycles at 0.5C	[4]
VG/Li_2S-C	1.84 mg cm^{-2}	890 mAh g^{-1} at 0.1C	~74% within 100cycles at 0.1C	[5]
Li_2S/FWNTs@G	1.0-1.5 mg cm^{-2}	980 mAh g^{-1} at 0.2C	~89% within 300cycles at 0.2C	[6]
Li_2S@C	3-3.5 mg cm^{-2}	971 mAh g^{-1} at 0.1C	~59% within 200cycles at 0.1C	[7]
Nano-Li_2S@C	2.8 mg cm^{-2}	652 mAh g^{-1} at 0.5C 470 mAh g^{-1} at 1C	~74% within 200cycles at 0.5C ~86% within 200cycles at 1C	[8]
Li_2S@C-Co-N	2.0 mg cm^{-2}	1137 mAh g^{-1} at 0.2C	~82% within 300cycles at 0.2C	[9]
Al_2O_3-Li_2S-GS	1.2-1.5 mg cm^{-2}	728 mAh g^{-1} at 0.5C	~88% within 300cycles at 0.5C	[10]
Li_2S@$LiTiO_2$	1.2 mg·cm^{-2}	~732 mAh g^{-1} at 0.5C ~606 mAh g^{-1} at 1C	~97% within 200cycles at 0.5C ~88% within 400cycles at 0.5C ~94% within 400cycles at 1C	This work
Li_2S@$LiTiO_2$	2.5 mg·cm^{-2}	~566 mAh g^{-1} at 0.5C	~83% within 400cycles at 0.5C	This work
Li_2S@$LiTiO_2$	4.8 mg·cm^{-2}	~408 mAh g^{-1} at 0.5C	~92% within 200cycles at 0.5C	This work

Computational Details

Adsorption energies were computed using DFT optimized structures and energies. All calculations were performed with CP2K v4.1 using PBE(D3BJ) functional and DZVP-MOLOPT-SR-GTH basis set [11-17] with a 600 Ry plane wave energy cutoff. Geometries were converged to a max change in atomic positions between steps of 0.0005 au. The other values were left at their defaults.

Prior to performing surface calculations, cell volume and angles of the bulk material were relaxed with the method above. The TiO_2 starting structure was taken from Howard, Sabine, and Dickson,[18] while $LiTiO_2$ structure was taken from the Materials Project database.[19] It is a calculated structure but has similar lattice dimensions and shape to that described in Borghols et al. and de Klerk et al.[20, 21] Both structures fall in the $I4_1/amd$ space group. According to de Klerk and coworkers, this form of $LiTiO_2$ is stable above a lithiation fraction of 0.96 (x in Li_xTiO_2). The surface forms a series of ridges, each terminating in a Li-O-Li-O pattern with a spacing of ~4 Å between Li-(O)-Li and O-(Li)-O. As a point of reference, the S-S bond in polysulfides is ~2.2 Å.

Slabs cut along the (1 0 1)-facet were prepared with the aid of the VESTA software.[22] 30 Å of vacuum was added between surfaces to minimize their interaction with periodically replicated images. Additionally, surface dipole corrections were applied along the surface normal axis. Extended and collapsed Li_2S_x (x = 1, 2, 4, 6, 8) polysulfide chains were generated with Avogadro v1.2.0 and optimized in the same unit cell as the surface to avoid errors with mismatched numbers of plane waves.[23] The values reported consider only the most optimal energies obtained over all cases. Only the initial fragmentation/dissociation step was investigated for Li_2S_X (x=4,6,8) on $LiTiO_2$, the follow up reactions were not investigated but subsequent decomposition up to Li_2S is likely.

Notes and References

1. N. Wang, N. Zhao, C. Shi, E. Liu, C. He, F. He and L. Ma, *Electrochimica Acta*, 2017, **256**, 348-356.
2. S. Liang, C. Liang, Y. Xia, H. Xu, H. Huang, X. Tao, Y. Gan and W. Zhang, *Journal of Power Sources*, 2016, **306**, 200-207.
3. G. Zhou, J. Sun, Y. Jin, W. Chen, C. Zu, R. Zhang, Y. Qiu, J. Zhao, D. Zhuo, Y. Liu, X. Tao, W. Liu, K. Yan, H. R. Lee and Y. Cui, *Advanced Materials*, 2017, **29**, 1603366-n/a.
4. G. Zhou, E. Paek, G. S. Hwang and A. Manthiram, *Advanced Energy Materials*, 2016, **6**, 1501355-n/a.
5. D. Wang, X. Xia, Y. Wang, D. Xie, Y. Zhong, J. Wu, X. Wang and J. Tu, *Chemistry – A European Journal*, 2017, **23**, 11169-11174.
6. Y. Chen, S. Lu, J. Zhou, W. Qin and X. Wu, *Advanced Functional Materials*, 2017, **27**, 1700987-n/a.
7. X. Li, M. Gao, W. Du, B. Ni, Y. Wu, Y. Liu, C. Shang, Z. Guo and H. Pan, *Journal of Materials Chemistry A*, 2017, **5**, 6471-6482.
8. T. Yang, X. Wang, D. Wang, S. Li, D. Xie, X. Zhang, X. Xia and J. Tu, *Journal of Materials Chemistry A*, 2016, **4**, 16653-16660.
9. J. He, Y. Chen, W. Lv, K. Wen, C. Xu, W. Zhang, Y. Li, W. Qin and W. He, *ACS Nano*, 2016, **10**, 10981-10987.
10. Y. Chen, S. Lu, J. Zhou, X. Wu, W. Qin, O. Ogoke and G. Wu, *Journal of Materials Chemistry A*, 2017, **5**, 102-112.
11. S. Grimme, J. Antony, S. Ehrlich and H. Krieg, *The Journal of chemical physics*, 2010, **132**, 154104.
12. S. Grimme, S. Ehrlich and L. Goerigk, *Journal of computational chemistry*, 2011, **32**, 1456-1465.
13. J. P. Perdew, K. Burke and M. Ernzerhof, *Physical review letters*, 1996, **77**, 3865.
14. S. Goedecker, M. Teter and J. Hutter, *Phys Rev B Condens Matter*, 1996, **54**, 1703-1710.
15. C. Hartwigsen, S. Goedecker and J. Hutter, *Phys Rev B*, 1998, **58**, 3641-3662.
16. J. Hutter, M. Iannuzzi, F. Schiffmann and J. VandeVondele, *Wiley Interdisciplinary Reviews: Computational Molecular Science*, 2014, **4**, 15-25.

17. J. VandeVondele and J. Hutter, *The Journal of chemical physics*, 2007, **127**, 114105.
18. C. J. Howard, T. M. Sabine and F. Dickson, *Acta Crystallogr B*, 1991, **47**, 462-468.
19. A. Jain, S. P. Ong, G. Hautier, W. Chen, W. D. Richards, S. Dacek, S. Cholia, D. Gunter, D. Skinner, G. Ceder and K. A. Persson, *APL Materials*, 2013, **1**, 011002.
20. W. Borghols, D. Lützenkirchen-Hecht, U. Haake, E. Van Eck, F. Mulder and M. Wagemaker, *Physical Chemistry Chemical Physics*, 2009, **11**, 5742-5748.
21. N. J. J. de Klerk, A. Vasileiadis, R. B. Smith, M. Z. Bazant and M. Wagemaker, *Physical Review Materials*, 2017, **1**, 025404.
22. K. Momma and F. Izumi, *Journal of Applied Crystallography*, 2011, **44**, 1272-1276.
23. M. D. Hanwell, D. E. Curtis, D. C. Lonie, T. Vandermeersch, E. Zurek and G. R. Hutchison, *Journal of Cheminformatics*, 2012, **4**, 17.